SPECIFIC AIMS

Cystic fibrosis (CF) is the most common lethal genetic disease in people of Caucasian descent. CF is caused by mutations in the cystic fibrosis transmembrane conductance regulator (CFTR) gene, leading to a buildup of thick mucus in the airways that reduces mucociliary clearance and makes CF patients more susceptible to bacterial infections. *Pseudomonas aeruginosa* is the leading cause of mortality in CF patients and colonizes most adult CF patients. Biofilm formation by *P. aeruginosa* allows for multi-drug resistance and evasion of host immune responses during chronic infections. *P. aeruginosa* produces three exopolysaccharides, Pel, Psl, and alginate, which are the main components of its biofilm matrix. Interestingly, a recent study examining the lung microbiota of CF patients concluded that the presence of streptococci within the CF lung was correlated with stable lung function and increased microbial diversity. The most prevalent streptococcus found in the CF lung was the oral commensal *Streptococcus salivarius*, which has demonstrated inhibitory effects against multiple pathogens and the ability to inhibit activation of the pro-inflammatory NF-κB pathway in human bronchial epithelial cells. NF-κB levels are naturally high in CF patients, contributing to chronic lung inflammation and subsequent tissue damage.

Our preliminary studies have revealed that *S. salivarius* biofilm formation is promoted by the *P. aeruginosa* exopolysaccharide Psl. Further, a *S. salivarius* maltose-binding protein (MalE) was demonstrated to be overexpressed during co-culture of *S. salivarius* with *P. aeruginosa*. Our findings combined with previous literature suggest that interactions between *S. salivarius* and *P. aeruginosa* may contribute to improved lung function by promoting increased lung microbial diversity and altering *P. aeruginosa* pathogenesis in the lung. Although *S. salivarius* is associated with CF lung stability and has demonstrated anti-inflammatory functions, no studies have examined *P. aeruginosa* and *S. salivarius* interactions within the CF lung. We will test the hypotheses that *P. aeruginosa* Psl and *S. salivarius* MalE interact to promote *S. salivarius* biofilm formation, and the presence of *S. salivarius* in the CF lung improves lung function by downregulating pro-inflammatory cytokines downstream of NF-κB produced in response to *P. aeruginosa* infection.

Aim 1. Determine the mechanism by which *P. aeruginosa* exopolysaccharide Psl promotes *S. salivarius* biofilm formation *in vitro*. *P. aeruginosa* exopolysaccharide Psl promotes *S. salivarius* biofilm formation. Additionally, the *S. salivarius* maltose-binding protein MalE is overexpressed when co-cultured with *P. aeruginosa*. We hypothesize that MalE interacts with Psl to promote *S. salivarius* biofilm formation by either directly binding to Psl or facilitating the breakdown and metabolism of Psl. To test whether MalE binds to Psl, we will perform whole cell ELISA with wildtype and *malE*-deficient *S. salivarius* strain K12 to observe whether purified Psl isolated from *P. aeruginosa* strain PAO1 can bind to these cells. We will also examine co-localization of *S. salivarius* and Psl via confocal microscopy and assess the binding ability of purified MalE and Psl via isothermal titration calorimetry, a technique that measures changes in heat to determine binding kinetics of two molecules. To test if MalE plays a role in Psl metabolism, we will culture wildtype and *malE*-deficient *S. salivarius* in minimal media with purified Psl as the sole carbon source.

Aim 2. Determine the impact of *S. salivarius* on *P. aeruginosa* pathogenesis and host inflammatory response *in vivo*.

2A: Determine whether Psl enhances *S. salivarius* colonization in a novel rat model of co-infection. We will develop a rat model of co-infection based on a previous co-infection model created in our lab of *P. aeruginosa* and the oral commensal *Streptococcus parasanguinis* that allows us to examine interspecies interactions. We will infect rats intranasally with *S. salivarius* followed by *P. aeruginosa* eight hours later, as *S. salivarius* typically colonizes the airway before *P. aeruginosa*. We will quantify and compare *S. salivarius* colony-forming units after co-infection with wildtype and Psl-deficient *P. aeruginosa*. Additionally, we will assess co-localization of Psl and *S. salivarius* in rat lung sections via confocal laser microscopy using Psl and *S. salivarius* specific lectins.

2B: Determine whether *S. salivarius* downregulates *P. aeruginosa*-induced NF-kB activation, leading to less tissue damage in the CF rat lung. CF patients infected with *P. aeruginosa* experience episodes of respiratory exacerbation characterized by a large inflammatory response, including elevation of various pro-inflammatory cytokines. *S. salivarius* has been shown to downregulate the NF-κB pathway, which induces the production of many pro-inflammatory cytokines, including IL-1, IL-6, and TNF-α. *S. salivarius* has also been shown to downregulate IL-8 that is produced in response to *P. aeruginosa* infection *in vitro*. We will measure neutrophil recruitment and cytokines IL-1α, IL-1β, IL-6, IL-8, and TNF-α after *P. aeruginosa* infection of rats with and without *S. salivarius* via differential staining and multiplex cytokine assays, respectively. We will also examine immune cell infiltration and tissue damage via histological staining after co-infection and *P. aeruginosa* mono-infection.

Impact: Although many bacterial species colonize the CF lung, *P. aeruginosa* is largely studied as an isolated infection. Studying *P. aeruginosa* in the context of polymicrobial communities and learning how other species impact *P. aeruginosa* pathogenesis could aid in the development of non-antibiotic therapies for this highly antibiotic-resistant pathogen.

SIGNIFICANCE

Cystic fibrosis (CF) is a genetic disorder caused by mutations in the cystic fibrosis transmembrane conductance regulator (CFTR) gene, which codes for a chloride ion transporter. Defective ion transport caused by CFTR mutations lead to dehydration of the airway surface liquid in the lungs (1). Patients then accumulate thick mucus in the lungs, and the inability to clear this mucus from the airways allows for bacterial infections to occur (2). The bacterial species *Pseudomonas aeruginosa* is the leading cause of death in cystic fibrosis patients (3). *P. aeruginosa* uses various strategies to cause persistent infections in the lung, including evasion of the host immune system, conversion to a mucoid phenotype, and biofilm formation (3). These mechanisms make this pathogen difficult to treat with antibiotics and allow for the development of lifelong chronic infections that lead to rapid lung deterioration and mortality (4). *P. aeruginosa* can also cause damage to the lungs by causing chronic inflammation through mechanisms such as activation of the pro-inflammatory NF-κB pathway (5). Cystic fibrosis patients already harbor naturally elevated NF-κB levels and increased neutrophil recruitment to the lungs, and P. aeruginosa further worsens this heightened inflammatory response (6-8).

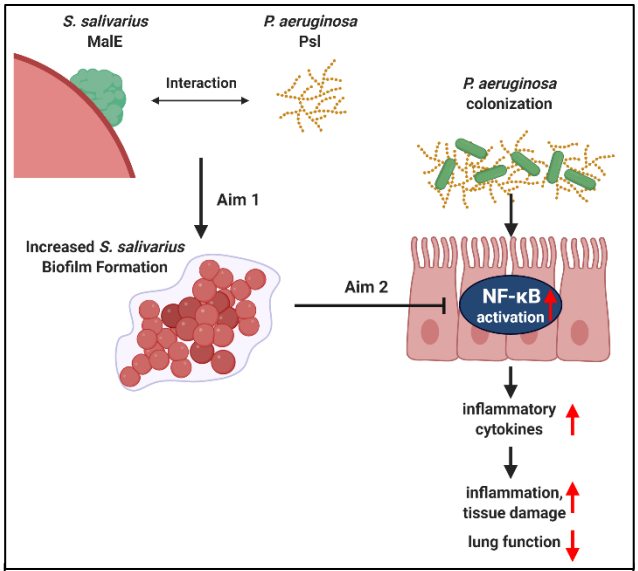

Figure 1: Schematic of the proposed mechanism. *S. salivarius* MalE interacts with the *P. aeruginosa* exopolysaccharide Psl to promote biofilm formation of *S. salivarius* (Aim 1). Promoted *S. salivarius* growth leads to downregulation of the NF-κB activation that is produced in response to *P. aeruginosa*, causing less inflammation and lung damage (Aim 2).

Biofilms are defined as communities of microbes that are attached to a surface and embedded in a protective extracellular matrix (9). The biofilm matrix of *P. aeruginosa* provides protection against multiple environmental stressors, including antibiotics, changes in pH, osmotic shock, and dehydration (10, 11). *P. aeruginosa* produces multiple exopolysaccharides that comprise its biofilm matrix. Non-mucoid strains *of P. aeruginosa*, which typically colonize the CF lung initially, produce the exopolysaccharides Pel and Psl, while mucoid strains are characterized by production of the exopolysaccharide alginate (12). Pel, Psl, and alginate play an important role in antimicrobial resistance by preventing penetration of antibiotics into the *P. aeruginosa* biofilm (13, 14). Pel is composed of *N*-acetylgalactosamine and *N*-acetylglucosamine, Psl is a branched polymer composed of mannose, rhamnose, and glucose, and alginate is a linear structure composed of D-mannuronic acid and L-guluronic acid residues (15, 16). Over the course of infection, non-mucoid strains will accumulate mutations in the anti-sigma factor *mucA* due to oxidative stress in the CF lung (17). *mucA* normally represses expression of the alginate operon, but when enough mutations accumulate, *mucA* functionality is lost and alginate is overexpressed, leading to the mucoid phenotype typically seen in the CF lung (12, 18).

There are many other microbes colonizing the CF lung in addition to *P. aeruginosa*. Research in recent years has focused on *P. aeruginosa* interactions with other microbes in the CF lung polymicrobial community (19, 20). For instance, *P. aeruginosa* has been found to synthesize glutamate from precursor molecules secreted by *Rothia mucilaginosa*, another common microbe found in the CF lung (21). Relevant to our study, the presence of oral streptococci in the lungs of CF patients was associated with increased lung stability and microbial diversity (22). Therefore, it is important to understand how these commensals are incorporated into the CF polymicrobial community and how they potentially promote better lung function in CF patients. We previously reported that the oral commensal *Streptococcus parasanguinis* adheres to the mucoid *P. aeruginosa* exopolysaccharide alginate using the cell surface adhesin BapA1, resulting in the promotion of *S. parasanguinis* biofilm formation (23). We are now examining the interactions between *P. aeruginosa* and *Streptococcus salivarius*, the most prevalent oral streptococcal species found within CF patients with stable lung function.

S. salivarius is a commensal bacterium that is an early colonizer of the oral cavity and has been shown to colonize the upper respiratory tract of children under two years of age (24). *S. salivarius* is approved in certain countries for use as a probiotic to prevent infection by *Streptococcus pyogenes*, the causative agent of Strep throat. The beneficial effects of *S. salivarius* are derived from the production of antimicrobial peptides which inhibit the growth of other streptococcal species (25, 26). *S. salivarius* in combination with *S. oralis* has been found to inhibit biofilm formation of multiple common upper respiratory tract pathogens, including *Streptococcus*

pneumoniae, *Staphylococcus aureus*, and *Staphylococcus epidermidis*, and *Moraxella catarrhalis* (27). While the impact of *S. salivarius* on the host immune system has not been thoroughly examined, multiple studies have highlighted its potential anti-inflammatory properties. Downregulation of the pro-inflammatory NF-κB pathway has been demonstrated after inoculation of human bronchial epithelial and intestinal epithelial cells with *S. salivarius* (28, 29). NF-κB represents a family of transcription factors which regulate a variety of genes involved in inflammatory responses (30). Additionally, pro-inflammatory cytokine IL-8 production induced by *P. aeruginosa* infection is significantly inhibited by *S. salivarius* colonization of epithelial cells (29).

Although *S. salivarius* is inhibitory against multiple pathogens, downregulates inflammatory responses, and is associated with CF lung stability, no studies have been performed to characterize the interactions of *P. aeruginosa* and *S. salivarius* and the impact of *S. salivarius* on the host immune response during *P. aeruginosa* infections. **The Aims proposed will determine 1.) how *S. salivarius* and *P. aeruginosa* physically interact within a biofilm to promote *S. salivarius* biofilm formation and 2.) how the presence of *S. salivarius* impacts the host inflammatory response and subsequent tissue damage during *P. aeruginosa* infection.**

INNOVATION

Until recently, *P. aeruginosa* and other pathogens have primarily been studied using single-species models of infection. Because the cystic fibrosis lung harbors an elevated amount of both pathogenic and commensal bacteria, the importance of studying *P. aeruginosa* in the context of polymicrobial communities needs to be recognized. Few studies have examined the interactions between *P. aeruginosa* and commensal bacteria in the lung. Although *S. salivarius* was the most prevalent streptococcal species found in a study that linked streptococci abundance to CF lung stability, **there are no studies examining interactions between *P. aeruginosa* and *S. salivarius* within a biofilm setting**. The development of a novel model of co-infection using CFTR knockout rats will allow for us to examine how *S. salivarius* incorporates into a *P. aeruginosa* biofilm in an environment that closely mimics the CF lung, as well as to thoroughly study the host immune response to *P. aeruginosa* infection in the presence of *S. salivarius*. This proposal will uncover unique mechanisms by which commensal bacteria such as *S. salivarius* modulate airway disease in CF patients.

APPROACH

Specific Aim 1. Determine the mechanism by which *P. aeruginosa* Psl promotes *S. salivarius* biofilm formation.

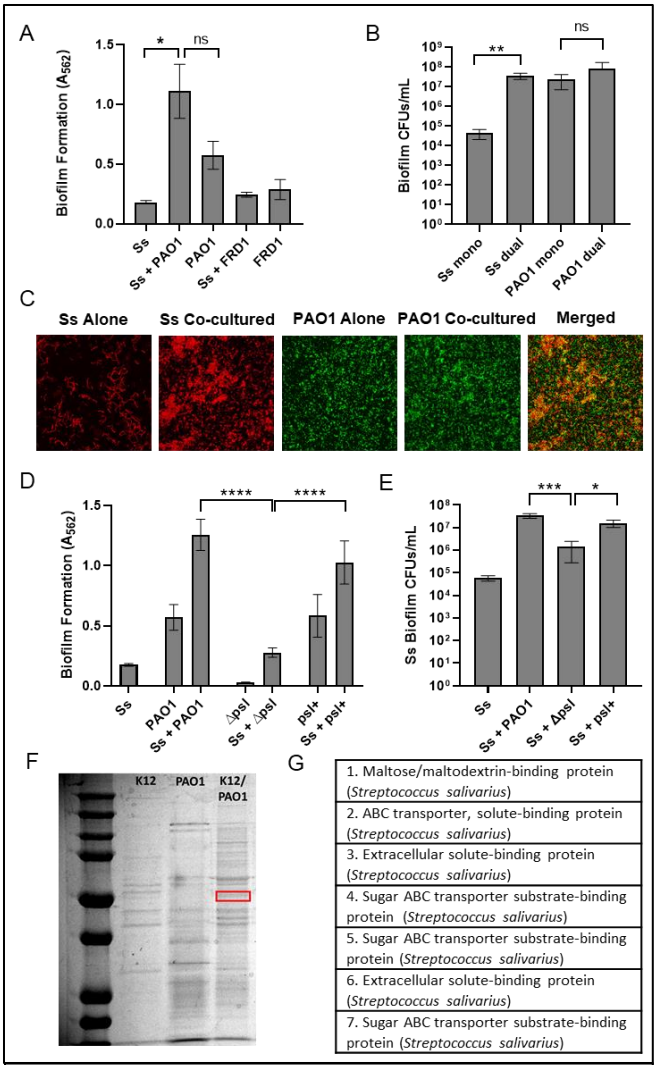

Figure 2: The *P. aeruginosa* exopolysaccharide Psl promotes *S. salivarius* biofilm formation. (A) *S. salivarius* (Ss) was co-cultured with either *P. aeruginosa* strain PAO1 or FRD1 in TSBYE with 1% sucrose then stained with crystal violet to measure biofilm biomass. **(B)** Quantification of Ss and PAO1 biofilm-forming cells was performed in a 6-hour 6-well mono- and dual-species model in synthetic CF sputum. **(C)** Confocal laser microscopy was performed on Ss and PAO1-GFP cultured in synthetic CF sputum. **(D)** Ss was co-cultured with WT PAO1, the Δ*pslA* mutant, and the Δ*pslA pslA*$^+$ complemented strains in TSBYE medium with 1% sucrose in a 96-well plate for 16 hours at 37℃ with 5% CO_2. Biofilm biomass was measured using crystal violet staining. **(E)** Quantification of Ss biofilm-forming cells after co-culturing with PAO1, PAO1Δ*pslA*, and PAO1 Δ*pslA pslA*$^+$ in a 6-hour 6-well model at 37℃ with 5% CO_2. **(F)** Ss and PAO1 were co-cultured in TSBYE with 1% sucrose to OD_{600} ~2.0. Whole cell lysate was run on an SDS-Page gel, and the protein band (highlighted in red) was sent to the UAB Mass Spectrometry Core for analysis. (G) Top gene candidates for mass spectrometry band (highlighted in red in Fig 1F). P-value: *≤0.05, **≤0.01, ***≤0.001,

Rationale and Preliminary Data: Our preliminary data show that in the presence of *P. aeruginosa*, *S. salivarius* biofilm cell number increases significantly. We first co-cultured *S. salivarius* strain K12 with an acute, non-mucoid strain of *P. aeruginosa* (PAO1) and a chronic, mucoid strain (FRD1). We then measured changes in biofilm

formation via crystal violet staining and found that co-culturing *S. salivarius* with PAO1 caused a significant increase in biofilm biomass (**Fig. 2A**). We enumerated colony forming units (CFUs) of the two-species biofilm and found that *S. salivarius* biofilm cell number significantly increased, while *P. aeruginosa* cell count did not (**Fig 2B**). We also confirmed this phenotype visually with confocal laser microscopy (**Fig. 2C**). Because biofilm formation only increases when *S. salivarius* is co-cultured with a non-mucoid strain of *P. aeruginosa*, and a major difference between mucoid and non-mucoid *P. aeruginosa* strains is their exopolysaccharide production, we hypothesized that Psl, the main exopolysaccharide produced by non-mucoid *P. aeruginosa* strain PAO1, promotes *S. salivarius* biofilm formation. Co-culture of *S. salivarius* with a Psl-deficient mutant of PAO1 (PAO1*ΔpslA*) caused a decrease in overall biofilm biomass (**Fig 2D**) and *S. salivarius* cell number (**Fig 2E**). *S. salivarius* biofilm cell number was restored when *pslA* was complemented back into PAO1*ΔpslA*, suggesting that the presence of Psl increased *S. salivarius* biofilm formation. Lastly, we observed the overexpression of a potential *S. salivarius* maltose-binding protein (MalE) after co-culture with *P. aeruginosa* via mass spectrometry (**Fig. 2F**). MalE is part of an ATP binding cassette (ABC) transporter complex that transports maltose and higher maltodextrins into cells and is located in the periplasmic space of Gram-negative bacteria such as *E. coli* (31). Although the localization of MalE in *S. salivarius* has yet to be characterized, MalE has been found on the surface of other Gram-positive bacteria (32). Because MalE binds to glucose polymers, and Psl is the only exopolysaccharide produced by *P. aeruginosa* that contains glucose within its structure (15), it is possible that MalE may bind to one or more of the sugars in Psl. Our lab has previously demonstrated that *Streptococcus parasanguinis*, another oral commensal implicated in CF lung stability, promotes its own biofilm formation by binding to the *P. aeruginosa* exopolysaccharide alginate via two of its surface proteins, BapA1 and Fap1 (23). Taken together, our findings lead us to hypothesize that MalE is responsible for enhanced biofilm formation of *S. salivarius* when co-cultured with *P. aeruginosa* due to interactions with Psl. We will test whether MalE may be directly binding to Psl, resulting in enhanced *S. salivarius* biofilm formation, or whether *S. salivarius* metabolizes Psl as a carbon source via the maltose/maltodextrin system. Alternatively, we will assess the interaction of Psl with other candidate *S. salivarius* proteins.

Experimental Design: We will first examine whether *S. salivarius* co-localizes with Psl via confocal laser microscopy after co-culturing of *S. salivarius* and *P. aeruginosa*. We will also examine co-localization of *S. salivarius* and purified Psl. Psl will be purified through a previously described technique in which Psl will be ethanol-precipitated from cultures of PAO1 *psl*+, a Psl-overproducing strain, then treated with DNase, RNase, and Proteinase K, and subsequently lyophilized (33). Using the confocal microscopy software NIS Elements, the two fluorescent signals will be plotted against one another on a scatterplot, and Pearson's correlation coefficient will be used to statistically quantify co-localization. Psl will be stained with a fluorescent FITC-conjugated Hippeastrum hybrid lectin, while *S. salivarius* will be stained with hexidium iodide, which stains Gram-positive bacteria and fluoresces red. To determine the role of MalE in promotion of *S. salivarius* biofilm formation, we will create a *malE* mutant of *S. salivarius* via allelic exchange mutagenesis in which we will insert a kanamycin resistance cassette in place of the *malE* gene. This mutant will then be co-cultured with *P. aeruginosa* in a 96-well plate in Tryptic Soy Broth with Yeast Extract (TSBYE) supplemented with 1% sucrose, and biofilm formation will be measured after 16-hour incubation via crystal violet staining and enumeration of CFUs per milliliter. To test the ability of *S. salivarius* to bind Psl, we will perform a whole-cell enzyme-linked immunosorbent assay (ELISA) in which microplates will be coated with *S. salivarius* cells. Coated plates will then be treated with purified Psl, and binding of Psl to *S. salivarius* will be detected via HRP-conjugated anti-Psl antibody. We will then assess the ability of *malE*-deficient *S. salivarius* to bind to purified Psl. Our positive control will be maltose, and our negative controls will be purified Pel and alginate because we have previously demonstrated that these exopolysaccharides do not promote *S. salivarius* biofilm growth (data not shown). We will also examine whether purified MalE can directly bind to purified Psl using isothermal titration calorimetry (ITC), a technique that measures binding affinity via heat that is absorbed or released during a binding event. To assess the ability of *S. salivarius* to metabolize Psl, we will grow wildtype and *malE*-deficient *S. salivarius* in M9 minimal media supplemented with Psl as the sole carbon source. Our positive control will be M9 supplemented with sucrose, a sugar that *S. salivarius* is known to metabolize, while our negative controls will be purified Pel and alginate. We will quantify CFUs of *S. salivarius* every two hours to assess the ability to metabolize Psl. This data will be analyzed in GraphPad Prism. Finally, we will perform crystal violet assays and quantify CFUs of *S. salivarius* co-cultured with non-mucoid isolates of *P. aeruginosa* collected from CF patients to determine if promotion of *S. salivarius* biofilm formation by *P. aeruginosa* is conserved among other *P. aeruginosa* isolates. All experiments will be performed in triplicate, and both crystal violet assays and CFU quantification will include three technical replicates per biological replicate.

Statistical Analysis: Student's t-tests will be used to analyze data in GraphPad Prism from crystal violet assays, CFU quantification, and ELISAs. A p-value of less than 0.05 will be considered statistically significant. ITC data will be collected and then be analyzed using the Origin software with the help of Dr. Champion Deivanayagam in the Department of Biochemistry and Molecular Genetics (*see letter of support*).

Expected Results and Alternative Outcomes: If *S. salivarius* binds to Psl, we would expect to see co-localization of *S. salivarius* and Psl with confocal laser microscopy. We would then expect to see binding of *S. salivarius* to purified Psl via whole-cell ELISA. If MalE binds to Psl, we should see a loss of this binding when performing an ELISA with purified Psl and *malE*-deficient *S. salivarius*. When examining binding of purified MalE to purified Psl via isothermal titration calorimetry, we would expect a change in heat to be detected, signaling that a binding event has occurred. Alternatively, we may not see co-localization of *S. salivarius* and Psl via microscopy. If *S. salivarius* and Psl do not co-localize, we would expect the increase in *S. salivarius* growth to be due to metabolism of the sugars in Psl, rather than by Psl binding. If this holds true, *S. salivarius* should be able to grow in minimal M9 media supplemented with Psl as the sole carbon source, and the growth curve should look similar to that of *S. salivarius* supplemented with sucrose. We would not expect *S. salivarius* to grow in the presence of purified Pel or alginate because our data suggests that these polysaccharides do not promote *S. salivarius* biofilm formation. If *malE* plays a role in Psl catabolism, we will see no growth of *malE*-deficient *S. salivarius* in M9 supplemented with Psl. If we instead found that *malE*-deficient *S. salivarius* also metabolizes Psl, we would conclude that a different catabolism pathway plays a role in Psl metabolism. *S. salivarius* constitutively expresses genes encoding the mannose-phosphotransferase (PTS) system. This system facilitates the uptake and breakdown of mannose, which is the most abundant sugar found in Psl. We will make mutants in genes essential for the function of the mannose-PTS system following a previously described protocol (34) and then assess the ability of these mutants to catabolize purified Psl in M9 minimal media. If neither MalE nor the mannose-PTS system are found to promote *S. salivarius* biofilm formation, we will perform transposon sequencing (Tn-seq) by creating a Mariner transposon library of *S. salivarius* with a protocol previously described (35). Mutants will then be co-cultured with *P. aeruginosa* to screen for a loss of the enhanced biofilm phenotype, and potential gene candidates will be identified via amplification of short nucleotide sequences adjacent to the Mariner transposon insert. Finally, if promotion of *S. salivarius* biofilm is consistent among non-mucoid *P. aeruginosa*, we would expect the promotion of *S. salivarius* biofilm formation by most non-mucoid clinical isolates that are co-cultured with *S. salivarius*. However, it is likely that the level of promotion will vary due to differing levels of Pel and Psl production in each isolate.

Specific Aim 2. Determine the impact of *S. salivarius* on *P. aeruginosa* pathogenesis and host inflammatory response *in vivo*.

Rationale and Preliminary Data: To examine whether *S. salivarius* impacts *P. aeruginosa* pathogenesis, we used *Drosophila melanogaster* as a model for co-infection and measured survival rates of *P. aeruginosa*-infected flies with and without *S. salivarius*. Fly survival was recorded for 10 days after infection. A significantly larger percentage of flies died after *P. aeruginosa* infection compared to those infected with both *P. aeruginosa* and *S. salivarius*, indicating that the presence of *S. salivarius* may protect flies from killing by *P. aeruginosa* (**Fig. 3**). These results have prompted us to further study *in vivo* interactions between *S. salivarius* on *P. aeruginosa* and their impact on *P. aeruginosa* pathogenesis and consequent damage to host tissues. Data from our lab show that Psl promotes *S. salivarius* biofilm formation (**Fig. 2**), and it is known that streptococci in the lung are associated with increased lung stability (15). Because *S. salivarius* is associated with lung stability, it is important that we understand factors that may promote or sustain colonization of *S. salivarius* in the lung. To study *in vivo* interspecies interactions, we will develop a novel rat model of co-infection with *S. salivarius* strain K12 and *P. aeruginosa* strain PAO1, which will be performed in Aim 2A. Studies suggest that *S. salivarius* and other oral streptococci are passed from mother to infant only days after birth (36). These oral streptococci are found colonizing the upper respiratory tract of children under two years of age (24). *P. aeruginosa* does not typically colonize CF patients early after birth; prevalence of *P.*

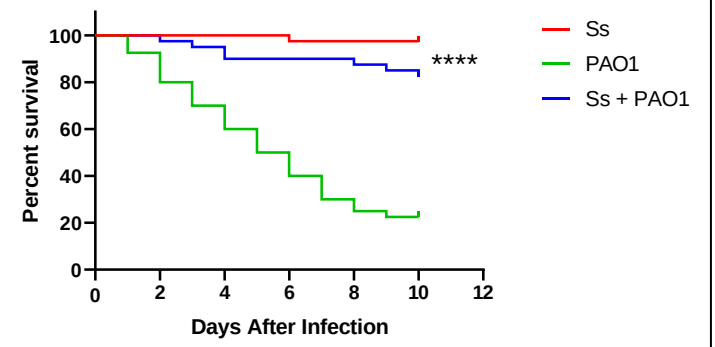

Figure 3: *S. salivarius* protects *Drosophila melanogaster* from killing by *P. aeruginosa*. *Drosophila melanogaster* were infected with *S. salivarius* and *P. aeruginosa* (PAO1). Curves represent 2 biological replicates with 4 technical replicates, n=10 per replicate. ****P <0.0001

aeruginosa in CF patients increases with age, eventually colonizing the majority of patients by adulthood (37). Therefore, we will develop a co-infection model in which *S. salivarius* colonizes the lung before *P. aeruginosa*. Wildtype and CFTR knockout Sprague Dawley rats will be used for this model of co-infection, provided by Dr. Susan Birket in the Division of Pulmonary, Allergy & Critical Care Medicine (*see letter of support*). Our lab has developed a successful co-infection rat model of *S. parasanguinis*, another oral commensal, and *P. aeruginosa* in which rats are infected intranasally with *S. parasanguinis* overnight culture and then infected intranasally with *P. aeruginosa* 8 hours later (data not shown). We will develop a model of *S. salivarius* and *P. aeruginosa* infection that closely mimics the co-infection model that our lab developed previously.

The large inflammatory response induced by *P. aeruginosa* infections is associated with further damage of the CF lung and poorer prognosis. CF patients colonized with *P. aeruginosa* experience respiratory exacerbation episodes characterized by a large inflammatory response with increased levels of pro-inflammatory cytokines IL-1, IL-6, IL-8, and TNF-α (38). Many probiotics, including *Bifidobacterium* and *Lactobacillus* species, downregulate the pro-inflammatory NF-κB pathway and IL-8 production in epithelial cells (39, 40). *S. salivarius* has been shown to inhibit the translocation of the NF-κB subunit p65 to the nucleus in human bronchial epithelial cells (HBECs), ultimately preventing NF-κB activation. NF-κB is a protein complex that stimulates the production of pro-inflammatory cytokines such as IL-1, IL-6, and TNF-α through regulation of transcription (30). The same study also demonstrated that *S. salivarius* inhibited both baseline secretion of IL-8 by HBECs and IL-8 production in response to *P. aeruginosa* infection. Another study found that supernatants from multiple *S. salivarius* strains significantly reduced NF-κB activation in intestinal epithelial cells, and two of these strains produced a compound smaller than 3 kDa of peptidic nature that directly inhibited NF-κB activation (41). Lastly, treatment of pharyngeal epithelial cells with *S. salivarius* strain K12 caused decreases in baseline secretion of IL-6, IL-8, and TNF-α, while other *S. salivarius* strains varied in immunomodulatory effects (42). Overall, our preliminary data has led us to hypothesize that 1.) Psl enhances colonization of *S. salivarius* in the CF rat lung, and 2.) *S. salivarius* inhibits the pro-inflammatory host immune response to *P. aeruginosa* via NF-κB inhibition, thus decreasing lung tissue damage in a rat model of infection. To test our hypotheses, we will co-infect rats with *S. salivarius* and either wildtype or Psl-deficient *P. aeruginosa* and compare *S. salivarius* CFUs after 24 hours. We will also survey production of pro-inflammatory cytokines regulated by the NF-κB pathway, including IL-1α, IL-1β, IL-6, IL-8, TNF-α, and neutrophil recruitment in the lung after co-infection with *S. salivarius* and wildtype *P. aeruginosa*.

Aim 2A: Test the role of Psl in *S. salivarius* colonization using a novel rat model of co-infection.

Experimental Design: We will grow *S. salivarius* overnight in Todd-Hewitt Broth, spin down, then resuspend cells in phosphate-buffered saline (PBS). We will infect wildtype and CFTR KO rats intranasally with 100uL *S. salivarius* strain K12 culture per nostril (~$1x10^7$ CFU/mL). Eight hours post-infection, we will infect intranasally with 100uL *P. aeruginosa* strain PAO1 overnight culture resuspended in PBS (~$1x10^9$ CFU/mL). We will have a non-infected control group, as well as *S. salivarius* and *P. aeruginosa* mono-infected controls. We will use both male and female rats, and each group will contain 3 replicates of n = 4 rats. Animals will be sacrificed 24 hours post-infection, and bacterial burden of each species will be enumerated from homogenized lung tissue. To understand whether Psl enhances *S. salivarius* colonization in the lung, we will co-infect rats with *S. salivarius* and *P. aeruginosa* lacking Psl (PAO1*ΔpslA*) then compare *S. salivarius* homogenized tissue CFUs from the left lung to those of rats co-infected with wildtype *P. aeruginosa*. We will use both male and female rats, and each group will consist of n = 3 biological replicates and n = 4 rats per technical replicate. The right lung will be fixed in 10% neutral buffered formalin and sent to the UAB Pathology Core for embedding in paraffin wax. Mounted slides will be created from fixed lung tissue and will be fluorescently stained to examine co-localization of Psl and *S. salivarius* in the lung.

Statistical Analysis: Student's t-tests will be used to analyze data in GraphPad Prism from CFU quantification. A p-value of less than 0.05 will be considered statistically significant. Pearson's correlation coefficient will be used to statistically quantify co-localization of *S. salivarius* and *P. aeruginosa* via the NIS Elements software.

Expected Results and Alternative Outcomes: If our phenotype holds true, we expect to see a significant increase in *S. salivarius* bacterial burden from the *S. salivarius* mono-infected group to the dual-infected group, and we should see no significant change in *P. aeruginosa* bacterial burden. We would also expect to see an increase in colonization of both *S. salivarius* and *P. aeruginosa* in CFTR KO rats compared to wildtype rats due to decreased bacterial clearance abilities. It is possible that *P. aeruginosa* strain PAO1 may not adhere in the wildtype rat lung efficiently. Alternatively, we can inoculate with a range of different bacterial concentrations, or we can test other strains of non-mucoid *P. aeruginosa* that produce the same Psl-induced increase in *S. salivarius* biofilm formation for adherence in the rat lung. We can also inoculate agar beads with *P. aeruginosa* and then introduce them into the rat lung. This method of infection is commonly used and helps with retention of

P. aeruginosa in the lung (43). If we are unable to develop a rat model of dual-infection due to difficulties with bacterial clearance in the rat lung, we will develop an *in vitro* model of dual infection using airway epithelial cells. Co-infection of *P. aeruginosa* and *S. salivarius* has already been described in human bronchial epithelial cells by *Cosseau et al* (29). We could also co-infect an NF-κB reporter human epithelial pharyngeal cell line, which would allow us to directly measure NF-κB activation via changes in bioluminescence. While we would not be able to measure neutrophil recruitment with this model, we would still be able to measure pro-inflammatory cytokines downstream of NF-κB activation. If Psl enhances *S. salivarius* colonization in the rat lung, we would expect to see significantly higher *S. salivarius* CFUs after addition of wildtype PAO1 compared to PAO1*ΔpslA*. We would also expect to see co-localization of Psl and *S. salivarius* via fluorescent microscopy. Alternatively, if Psl does not promote *S. salivarius* colonization, we will stain for *P. aeruginosa* cells instead of Psl to look for general co-localization of *S. salivarius* and *P. aeruginosa* in the rat lung.

Aim 2B: Determine changes in the host NF-κB response to *P. aeruginosa* infection in the presence of *S. salivarius*

Experimental Design: We will include six infection groups for wildtype and CFTR KO rats as described in Aim 2A- an uninfected control group, *S. salivarius* K12 mono-infected control group, PAO1 mono-infected control group, PAO1*Δpsl* mono-infected control group, K12 and PAO1 wildtype dually-infected group, and a K12 and PAO1*Δpsl* dually-infected group. Each group will consist of n = 3 biological replicates and n = 4 rats per technical replicate. After 24 hours, BALF samples will be centrifuged to separate cells from the supernatant, and the supernatant will then be used to measure pro-inflammatory cytokines IL-1α, IL-1β, IL-6, MIP-2, and TNF-α via a custom multiplex Luminex assay. BALF cells will then be resuspended, mounted on slides using a cytocentrifuge, and stained differentially with eosin and methylene blue to detect and quantify neutrophils via microscopy. The right lung will be inflated, fixed in 10% neutral buffered formalin, and sent to the UAB Pathology Core for embedding in paraffin wax. We will then create mounted slides with fixed lung tissue which will undergo analysis by the Pathology Core, where hematoxylin and eosin staining will be used for histopathological analysis. Semi-quantitative scoring of lung sections will be performed by a board-certified veterinary pathologist in a blinded fashion. Scoring will be assigned based on the severity of neutrophil influx, a common marker of lung histopathology. Severity will be assessed using a scale of 0-4, where 0 corresponds to no observable neutrophils, 1 corresponds to ≤25%, 2 corresponds to 25-50%, 3 corresponds to 50-75%, and 4 corresponds to 75-100% of the section. Polymorphonuclear (PMN) cell density will be scored on a scale of 1 to 3, with 1 to representing mild, 2 representing moderate, and 3 representing severe. Severity and density scores will be multiplied to give final histopathology scores.

Statistical Analysis: Cytokine, neutrophil, and histopathological scoring data will be analyzed in GraphPad Prism using a one-way ANOVA with Tukey's multiple comparisons test for post-hoc analysis. A p-value of less than 0.05 will be considered statistically significant.

Expected Results and Alternative Outcomes: If *S. salivarius* suppresses inflammatory responses induced by the NF-κB pathway, we should see significantly less production of cytokines IL-1α, IL-1β, IL-6, and TNF-α in co-infected rats compared to those infected with *P. aeruginosa* only. We would also expect to see a decrease in MIP-2 and a consequent decrease in neutrophil recruitment because MIP-2, a murine homologue of IL-8, acts as a chemoattractant to recruit neutrophils to sites of infection. With this decrease in pro-inflammatory cytokines and neutrophils in the lung, we would expect to see significantly lower histopathological scores for the lung tissue in the co-infected group compared to the *P. aeruginosa*-infected group. Additionally, we would expect to see significantly higher levels of pro-inflammatory cytokines and neutrophil recruitment in the CFTR KO groups compared to all respective wildtype groups. If *S. salivarius* downregulates pro-inflammatory cytokine production, the increase in *S. salivarius* growth induced by the presence of Psl would further amplify this downregulation. Alternatively, we may not see a difference in inflammatory response between the co-infected and *P. aeruginosa*-infected groups. If this occurs, we will extend the infection time and observe cytokine and neutrophil responses at multiple time intervals to allow more time for an immune response to be formed against *P. aeruginosa*. We can also perform immunohistochemistry staining on infected lung tissue to look for changes in recruitment of other immune cells, which would give us a broader picture of the immune response.

Summary

The experiments proposed in these Aims will uncover mechanisms by which *S. salivarius* incorporates into the *P. aeruginosa* biofilm, a previously unexplored area of study, as well as how *S. salivarius* impacts the host response to *P. aeruginosa* and subsequent lung tissue damage. These findings will elucidate mechanisms by which commensals such as *S. salivarius* impact airway disease caused by pathogenic infections.